

John Bosco Habarulema

jhabarulema@sansa.org.za; J.Habarulema@ru.ac.za;

John.Habarulema@nwu.ac.za

South African National Space Agency

Department of Physics and Electronics, Rhodes University, RSA

Centre for Space Research, North West University, RSA



IRI and NeQuick-Improving the Representation of Real Time Ionosphere (29 Sept – 03 Oct, 2025)

A COSPAR Capacity Building Workshop



Fundamentals and Background

IRI model (Dieter Bilitza), NeQuick (Bruno Nava and Yenca Migoya-Orue), lonosondes (Ivan Galkin), Radio Occultation (Bruno Nava), ISR (Shunrong Zhang), GIMs for TEC (Andrzej Krankowski), Machine Learning (Yenca Migoya-Orue), ionospheric Variability (Lucilla Alfonsi)...

Ionospheric plasma frequency (f_p) is given by

$$\omega_p = 2\pi f_p = \sqrt{\frac{N_e e^2}{\epsilon m}}$$

Typical ionospheric N_e

- ▶ Typical ionospheric electron densities are $\sim 10^{11} 10^{12}$ electrons per m^3
- ▶ Plasma frequency is between 1-10 MHz === HF band
- ► For operational purposes, HF is the most affected by the ionosphere





Define 3D reconstruction

Fundamentally: this involves representation of an ionospheric (in our context) parameter (Ne) in 3 dimensions of space, time and altitude: and can be broadly done through three main approaches;

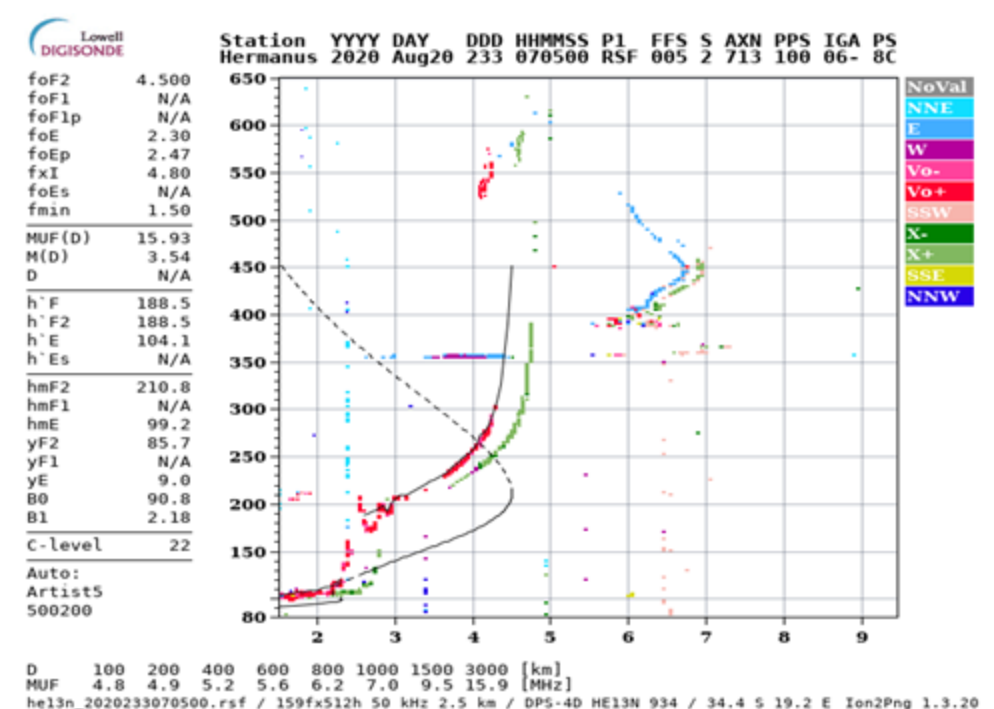
- 1. Theoretical: Solve the necessary hydrodynamic equations with some initial conditions. Requires experimental data for validation and usually computationally intensive
- 2. Empirical: Relies only on data to generate expected behaviour of any parameter under investigation. The output is as accurate as the what was used to develop the models.
- 3. Mixture of theoretical and empirical approaches sometimes known as semiempirical, etc and this would cater for some data assimilation techniques

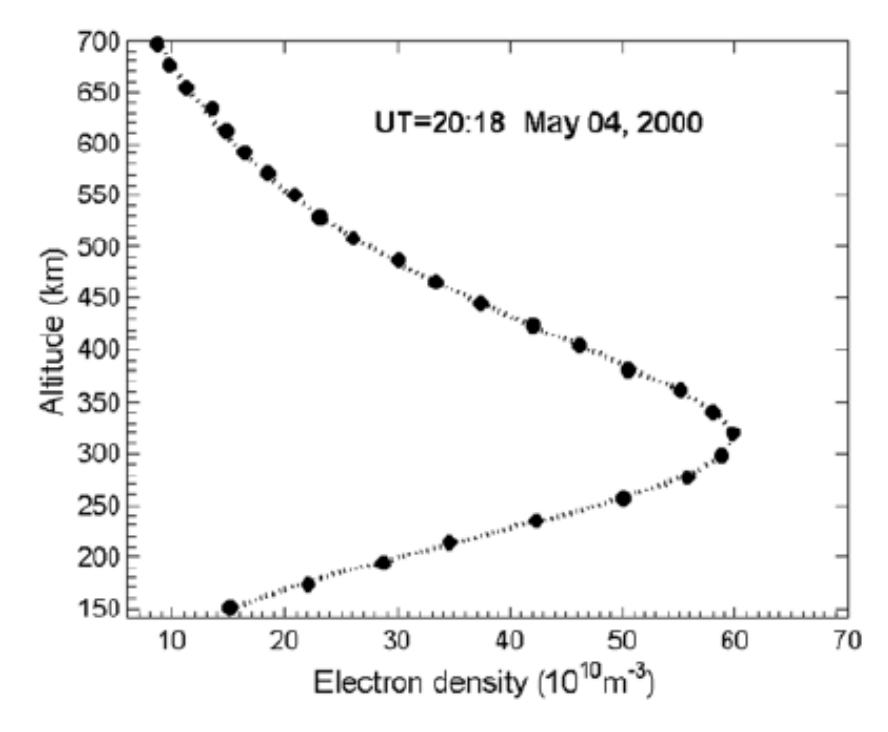




Challenges with ionospheric 3-D reconstruction

- Not many instruments are dedicated to this at all required altitudes, although most applications require reconstruction within 50-1000 km (ionosphere)
- Traditionally, ionospheric instrumentation include ionosondes and incoherent scatters (Figure used from Lei et al., 2005: Radio Science)



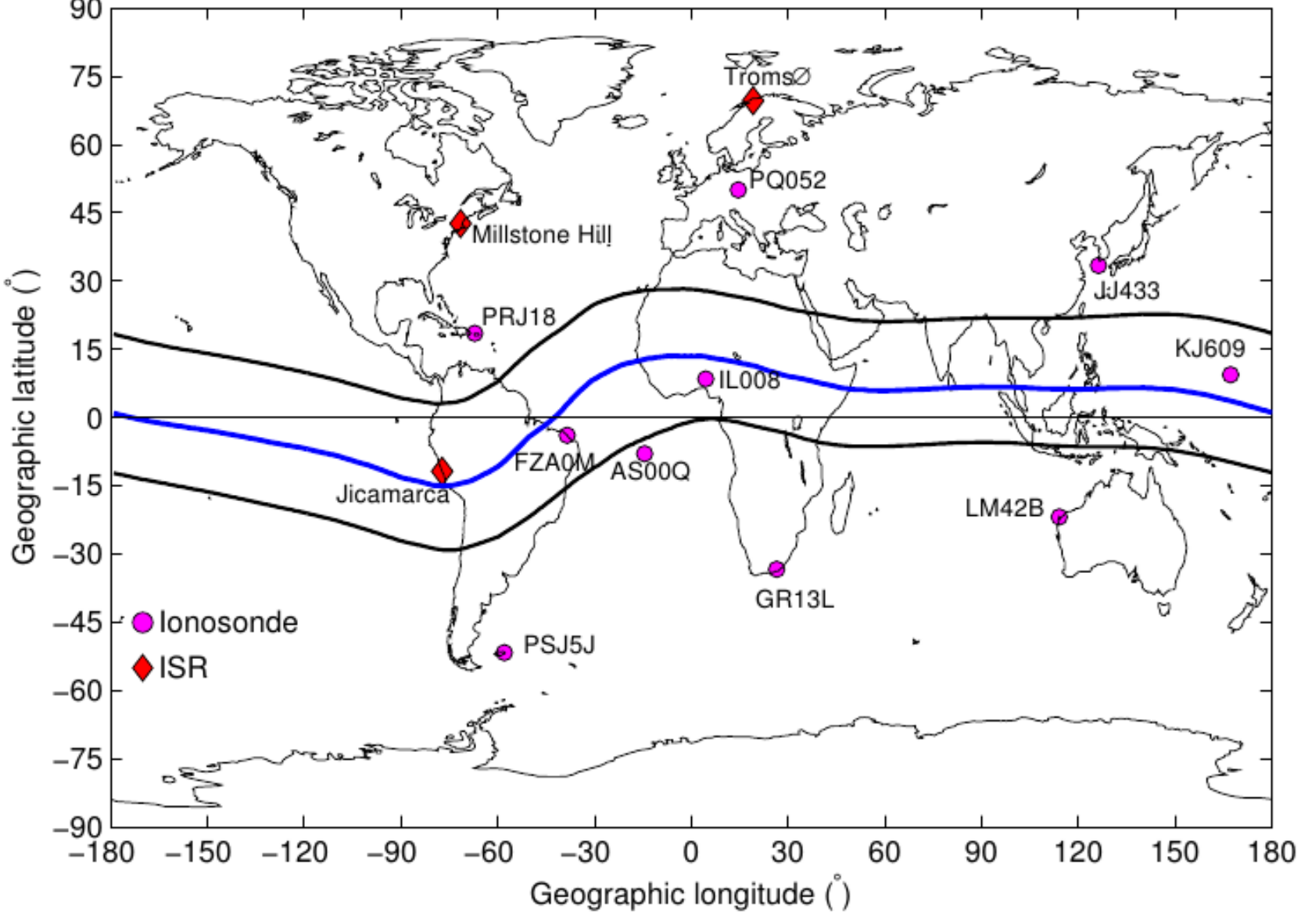






Currently operational ISRs? May be not a complete picture

Refer to the complete picture by Shunrong Zhang







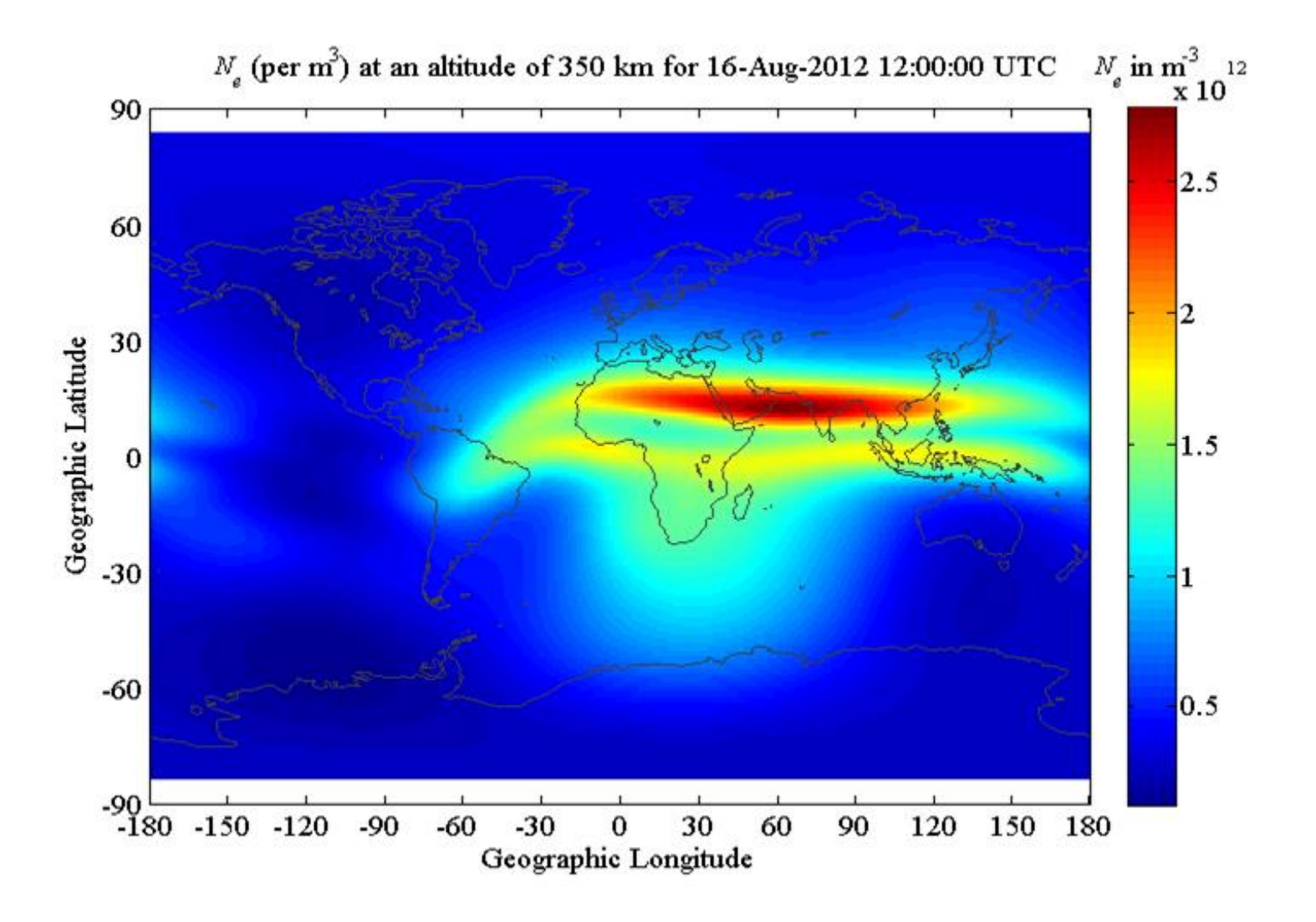
Global ionosonde network: slightly biased!







Among commonly used empirical models are IRI (Dieter's talk) and NeQuick (Bruno's and Yenca's talks)







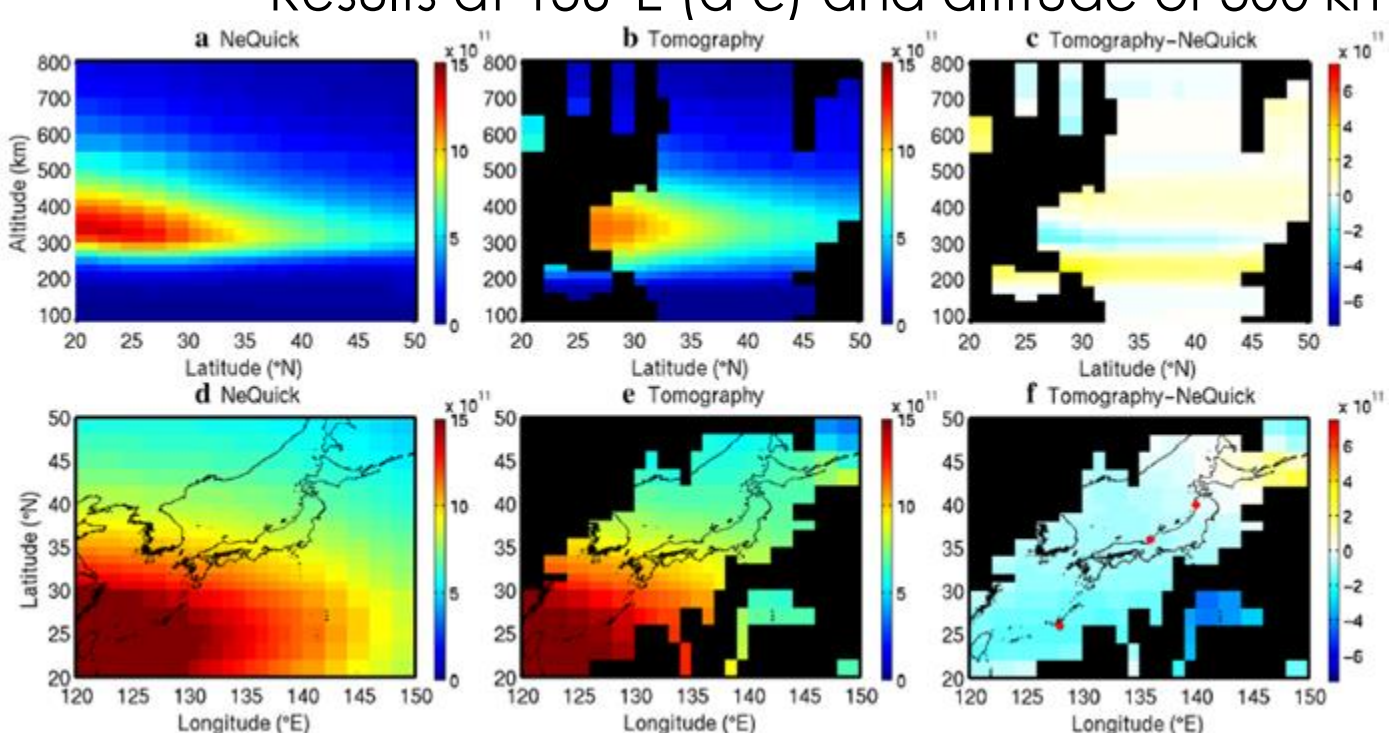
Ionospheric tomography

Spatial distribution of satellite data is usually not enough for accurately reconstructing electron density in 3-dimensions especially if the ground receivers are sparse.

Difficult inverse problem and in most cases requires iterative solving starting with an initial guess. Results may be sensitive to the assumed initial guesses

Reference: Chen et al., (2016): doi:10.1186/s40623-016-0412-6

Results at 136°E (a-c) and altitude of 300 km (d-f)





GPS satellite

GPS receiver

ionosphere

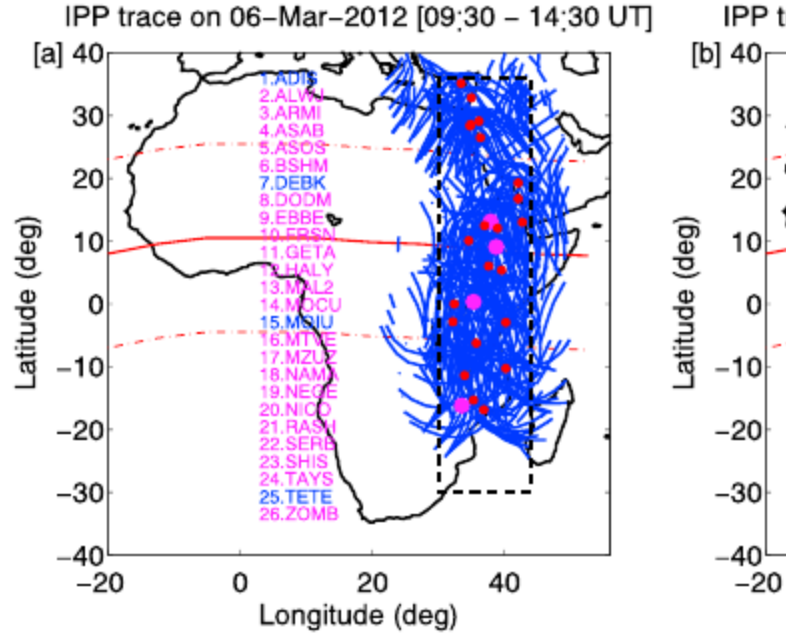
20,200 km

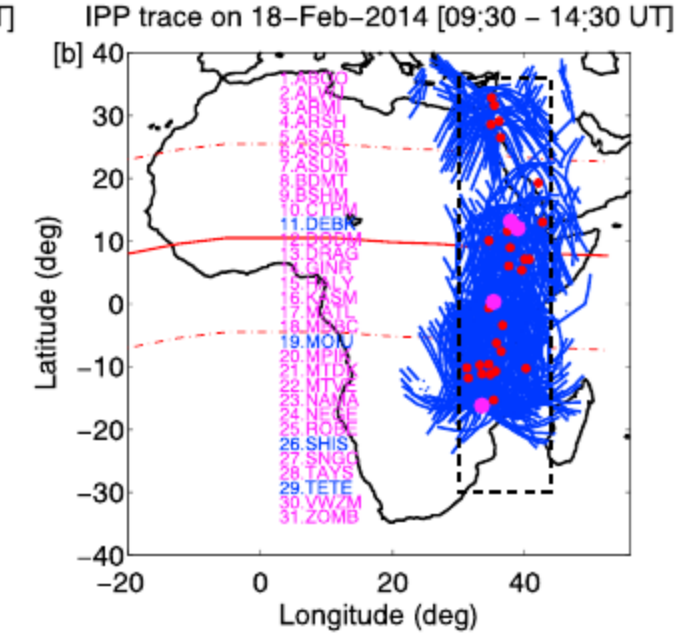
80 km



Very sparse ground-based sensors in some regions

Ionospheric tomography simply not possible over the African region









Radio Science

RESEARCH ARTICLE

10.1029/2017RS006499

Key Points:

- Performance evaluation of MIDAS compared with ANNs to reconstruct ionospheric total electron content during geomagnetic storms
- MIDAS performs 13% better than ANNs in African midlatitude region
- ANNs perform 24% better than MIDAS in African low-latitude region

Correspondence to:

J. C. Uwamahoro, juwamahoro@sansa.org.za

Reconstruction of Storm-Time Total Electron Content Using Ionospheric Tomography and Artificial Neural Networks: A Comparative Study Over the African Region

Jean Claude Uwamahoro^{1,2,3}, Nigussie M. Giday^{1,2,4}, John Bosco Habarulema^{1,2}, Zama T. Katamzi-Joseph^{1,2}, and Gopi Krishna Seemala⁵

¹ South African National Space Agency (SANSA), Space Science, Hermanus, South Africa, ² Department of Physics and Electronics, Rhodes University, Grahamstown, South Africa, ³ Department of Physics, College of Science and Technology, University of Rwanda, Kigali, Rwanda, ⁴ Ethiopian Space Science and Technology Institute (ESSTI), Addis Ababa, Ethiopia, ⁵ Indian Institute of Geomagnetism (IIG), Mumbai, India

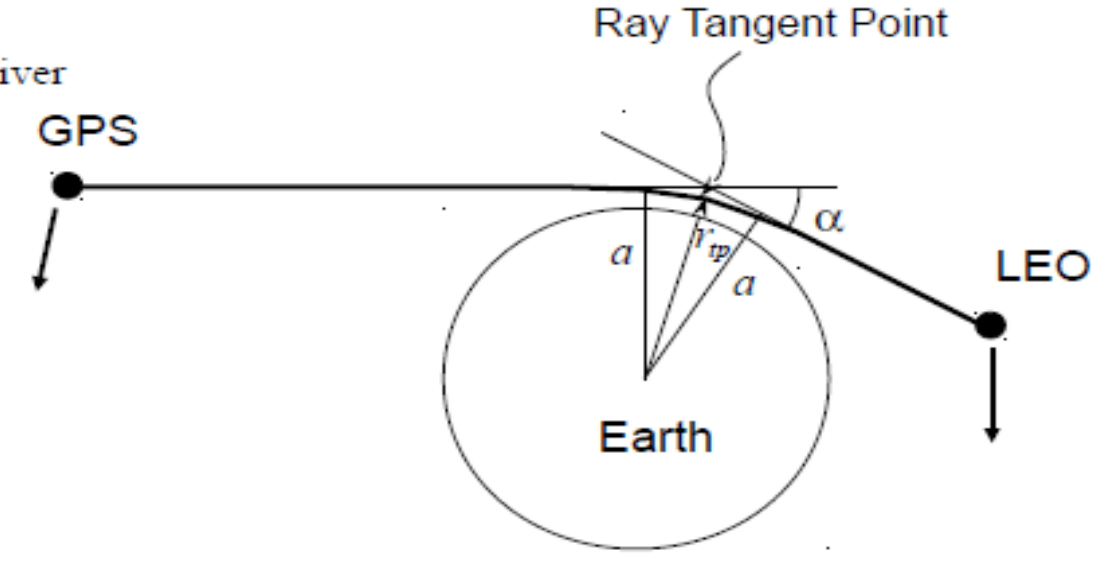




This led us to Radio Occultation sources

During a GPS occultation a GPS receiver in LEO 'sees' the GPS SV set or rise behind the Earth's limb while the signal slices through the atmosphere.

The GPS receiver in LEO observes the change of the delay of the signal between the GPS and the LEO that is related to slowing and bending of the signal path.



The change of the delay allows for reconstruction of the bending angle α and then the vertical refractivity profile at the ray tangent point

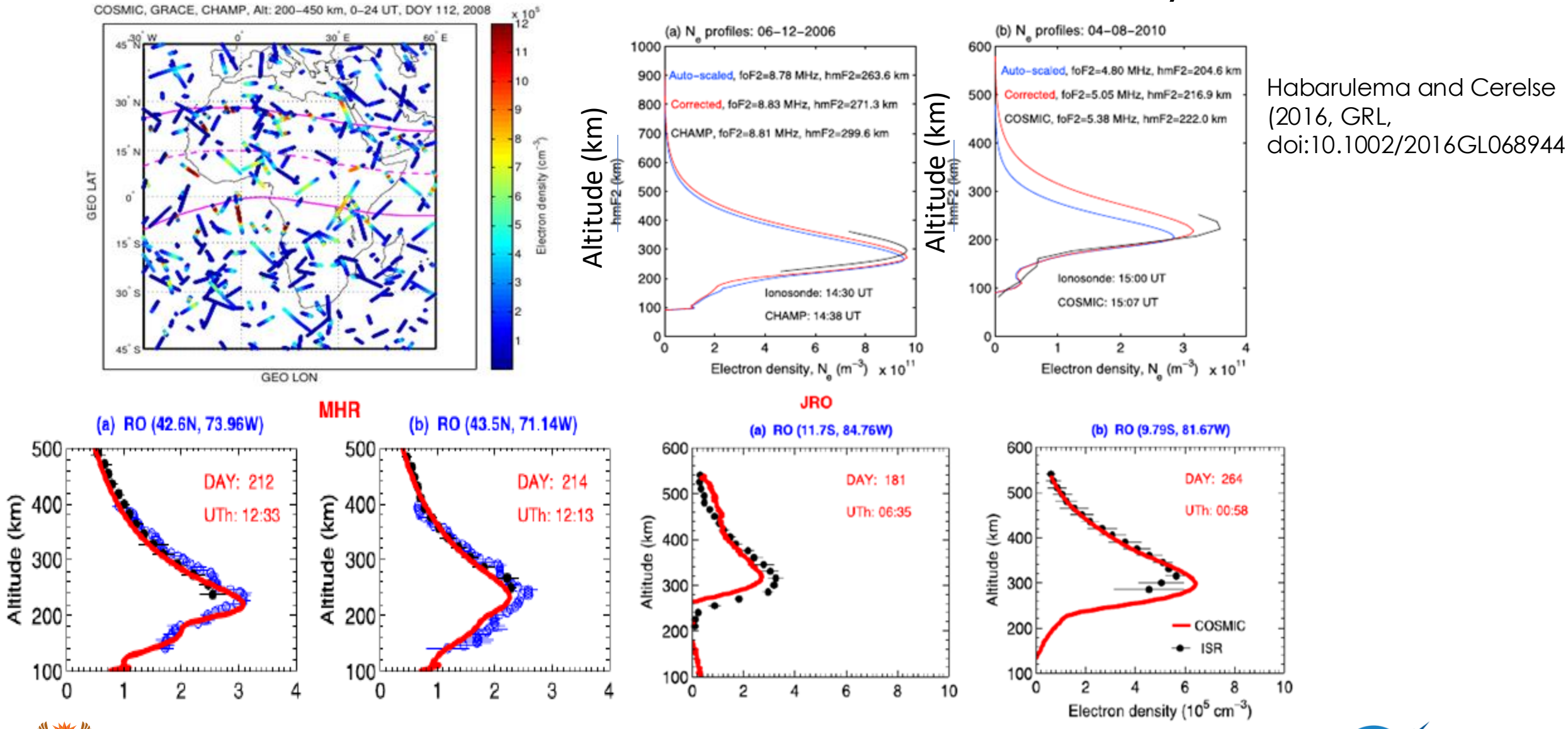
The refractivity allows for reconstruction of the pressure, temperature and humidity in the neutral atmosphere and electron density in the ionosphere

Reference: Kursinski et al., (2000): The GPS Radio Occultation Technique, Terr. Atmos. Ocean. Sci., 11 (1), 53–114





What has been chosen and why?

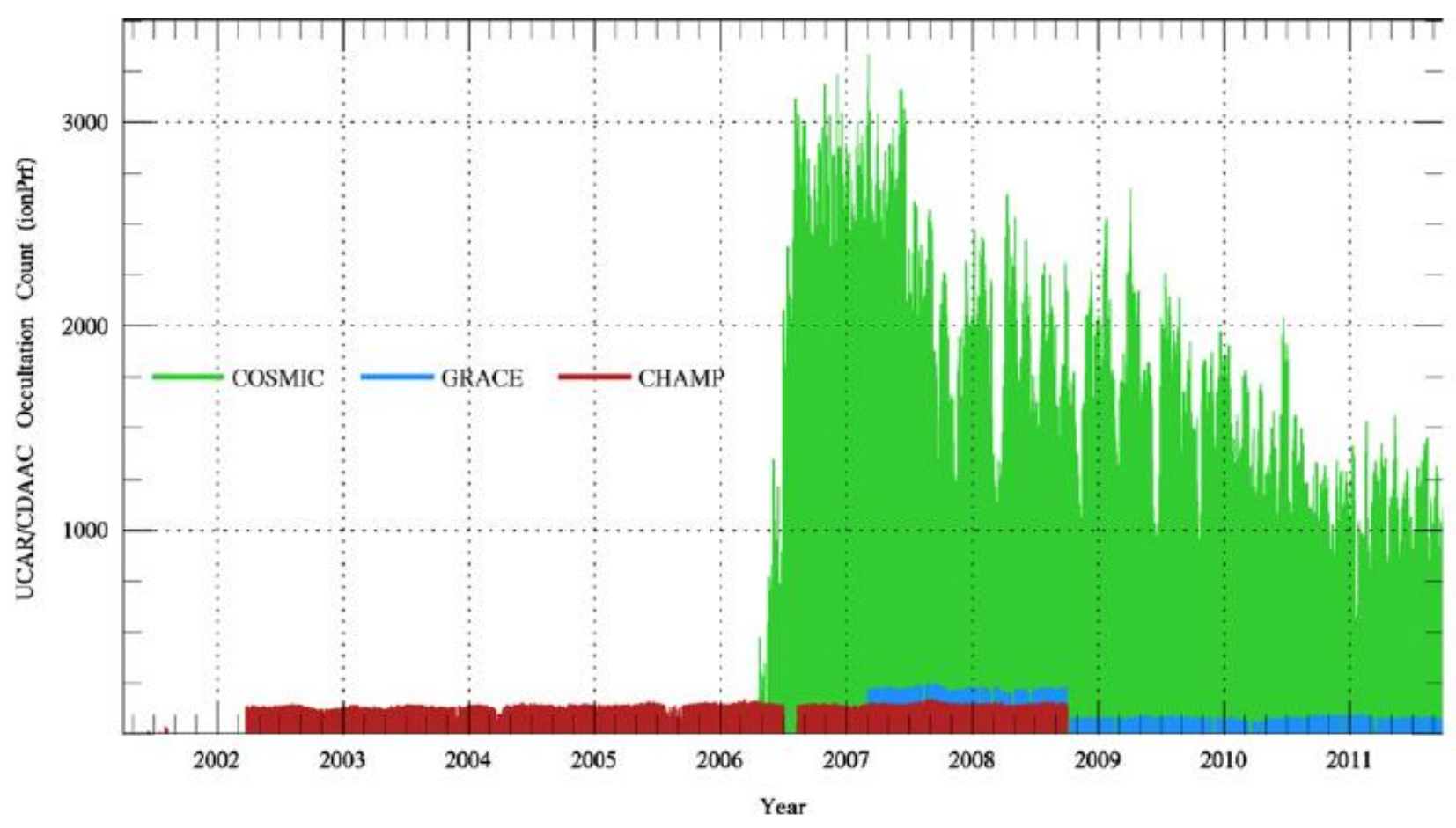


science & innovation

Science and Innovation REPUBLIC OF SOUTH AFRICA Citation: Lei, J., et al. (2007), Comparison of COSMIC ionospheric measurements with ground-based observations and model predictions: Preliminary results, J. Geophys. Res., 112, A07308, doi:10.1029/2006JA012240.



Data availability (2006-2019)



Yue et al., (2013): GNSS radio occultation (RO) derived electron density quality in high latitude and polar region: NCAR-TIEGCM simulation and real data evaluation; JASTP



COSMIC data used in this work consist of the second level data provided by the COSMIC Data Analysis and Archive Centre. These are the "ionprf" files that contain information about ionospheric electron density profiles.

http://cosmicio.cosmic.ucar.edu/cdaac/index.html

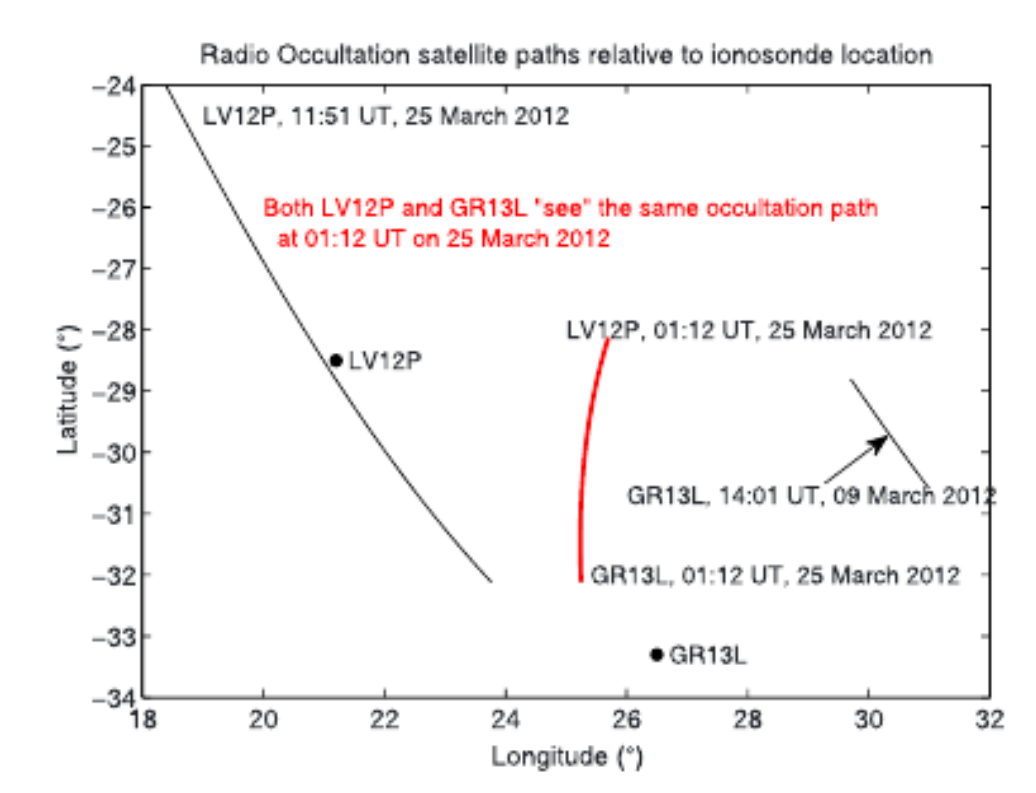
The model and driving inputs

Model is built solely using artificial neural networks with the following physical and geophysical inputs

- Diurnal variation
- Seasonal variation
- Solar activity (F10.7)
- Geomagnetic activity (Kp index)
- Latitude and longitude values at the point
- of the electron density value (this is important)
- Height/altitude corresponding to the electron density observation== this is what makes it 3-dimensional reconstruction model





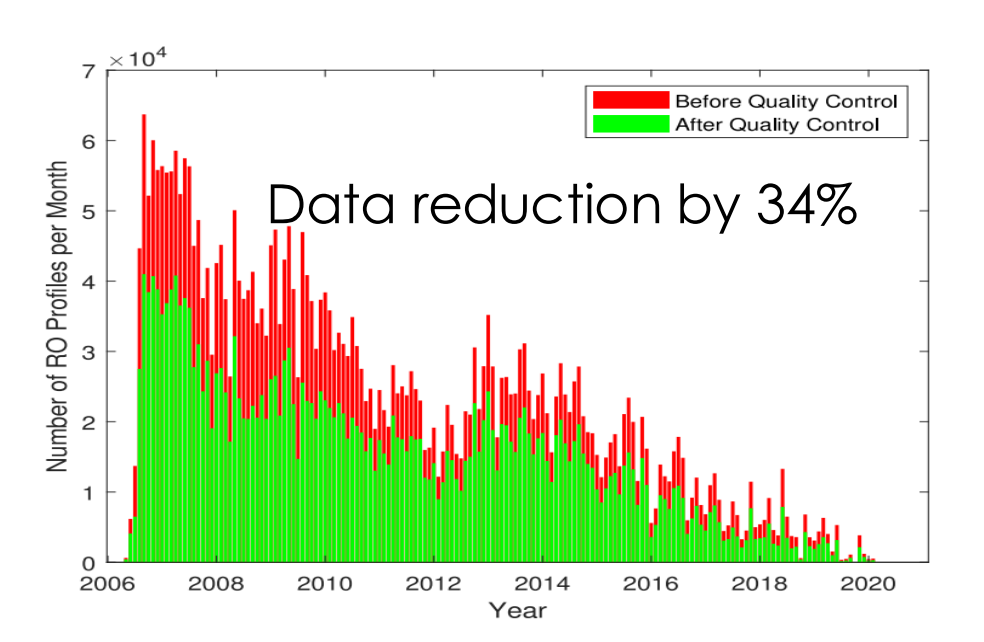


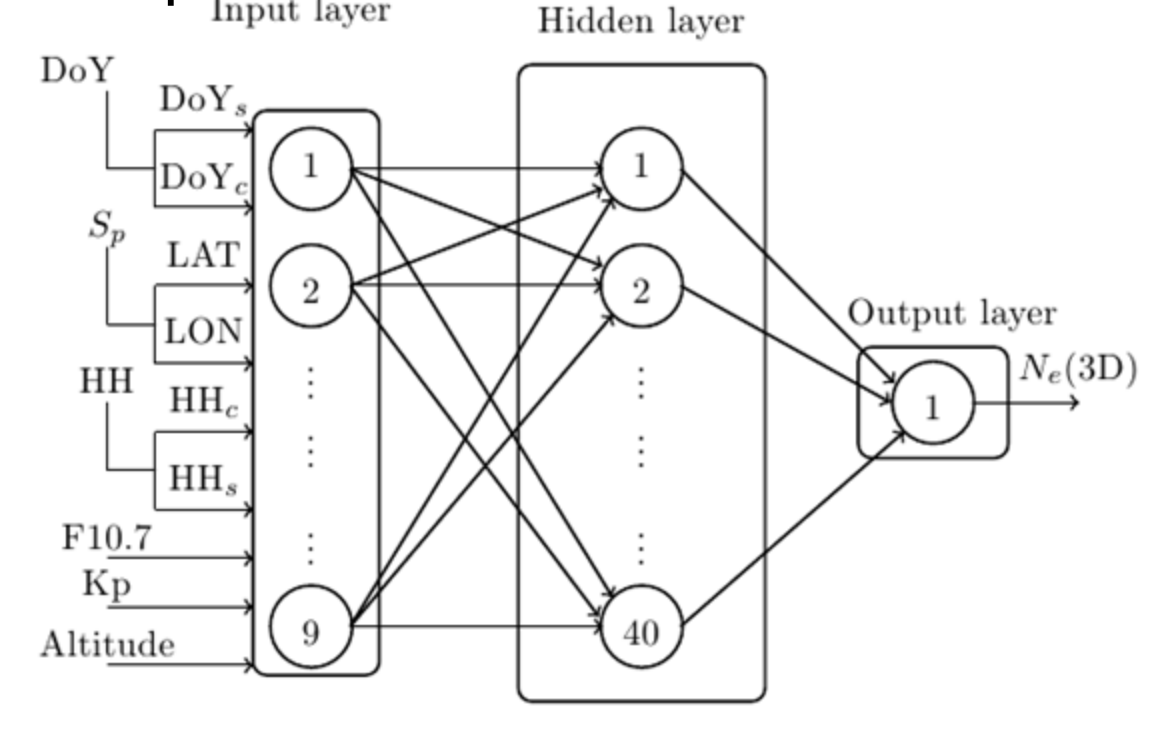


Data Quality Control and Model setup

During the electron density retrieval process, some profiles exhibit errors mainly related to negative values. To minimise such errors, we

- 1. Removed negative Ne values from all profiles
- 2. Eliminated entire profiles if negative Ne value appeared at altitudes greater than or equal to 100 km
- 3. All profiles with hmF2 outside the range of 200-550 km were removed





This process resulted into a database of global Ne profiles from 2006-2019 which is a huge dataset (2Bn data points) for computational purposes.

Divide data into spatial resolutions of 5 (latitude) by 15 (longitude) resulting into 864 sub-models which are combined to form one global model



Habarulema et al., (2021); A global 3-D electron density reconstruction model based on radio occultation data and neural networks; https://doi.org/10.1016/j.jastp.2021.105702



Brief introduction to neural networks

A technique for transforming a multi-dimensional input space $\mathbf{x} = \{x_1, x_2, ..., x_{N_i}\}$ of dimension N_i to an output single scalar y through input-output mapping process as (Camporeale, 2019)

$$y(\mathbf{x}) = \sum_{i=1}^{h} w_i A\left(\sum_{j=1}^{N_i} m_{ij} x_j + c_i\right)$$
 (3)

where A(.) is a continuous nonlinear function, usually known as activation function. Parameters w_i , m_{ij} are weights while c_i is the bias vector. These three are free parameters which requires optimisation by the NN.

- The input space x undergoes linear transformation by the weights m and bias vector c: Matrix-vector multiplication
- The resulting new vector from this linear transformation proceeds into the activation function A(.)
- The above two procedures are repeated h times, each with different weights m and biases c; where h is also a free parameter usually known as number of neurons.
- The h results of A(.) are finally linearly combined through the weights (w)

Major task is how to choose values of weights and biases; which is where training/learning algorithms come in.





The overall aim is to minimize the cost function

A machine learning or neural network algorithm seeks to solve an optimisation problem which is done by minimising the cost function selected before training.

Distance between observed and modelled values

A cost function specifically measures the dispersion between the observed and predicted parameter.

For a set of input-target pairs $(D = x^i, t^i)$, a neural network architecture N can be defined such that a cost function for the whole dataset under consideration can be defined (Mackay, 1992) as

$$E_D(D|w,N) = \sum_i \frac{1}{2} \{ y(x^i; w, N) - t^i \}^2$$
 (4)

where i is the label running over the pairs, w represent a set of values assigned to the connections in the network and $y(x^i; w, N)$ is the mapping from the input variables x to target parameter y.

Reference



Mackay (1992): A Practical Bayesian Framework for Backpropagation Networks, Neural Computation 4, 448-472



Strengths and weaknesses of Machine learning

Strengths

ML/NN algorithms/models perform much better than physics-based/theoretical models in nowcasting and forecasting. They are described as "universal approximators"

Weakness

It is really not understood why they work well. The input-output mapping process is described as a "black box". A number of people focus on making the algorithm either work or understandable.

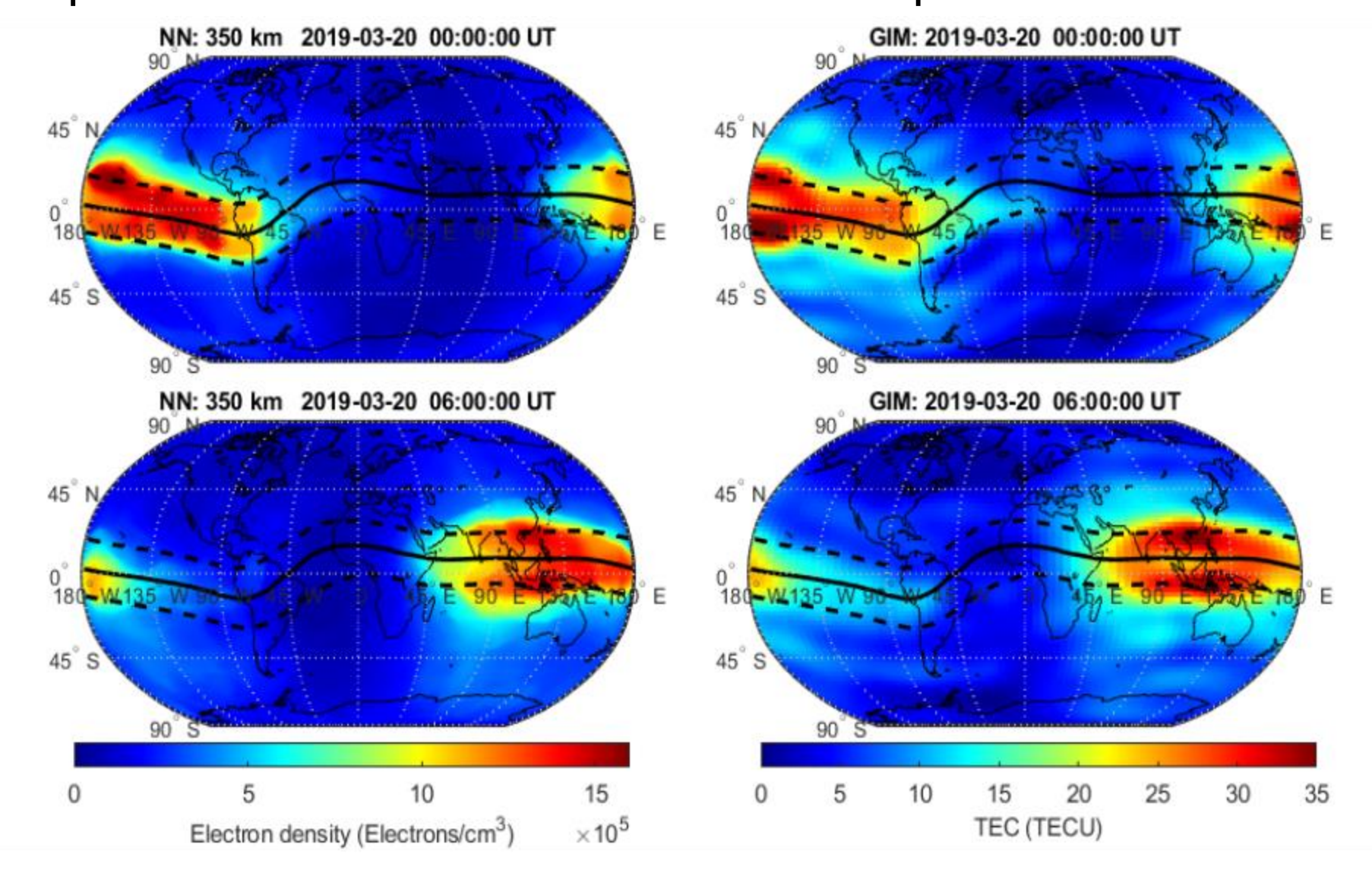
Qn: Should we not use them simply because we don't fully understand how they work??

Answer: We rely and trust our brain even when we have limited understanding about its functionality and working modalities (Reference: Castelvecchi (2016): Can we open the black box of AI? Nature News, 538(7623),20)





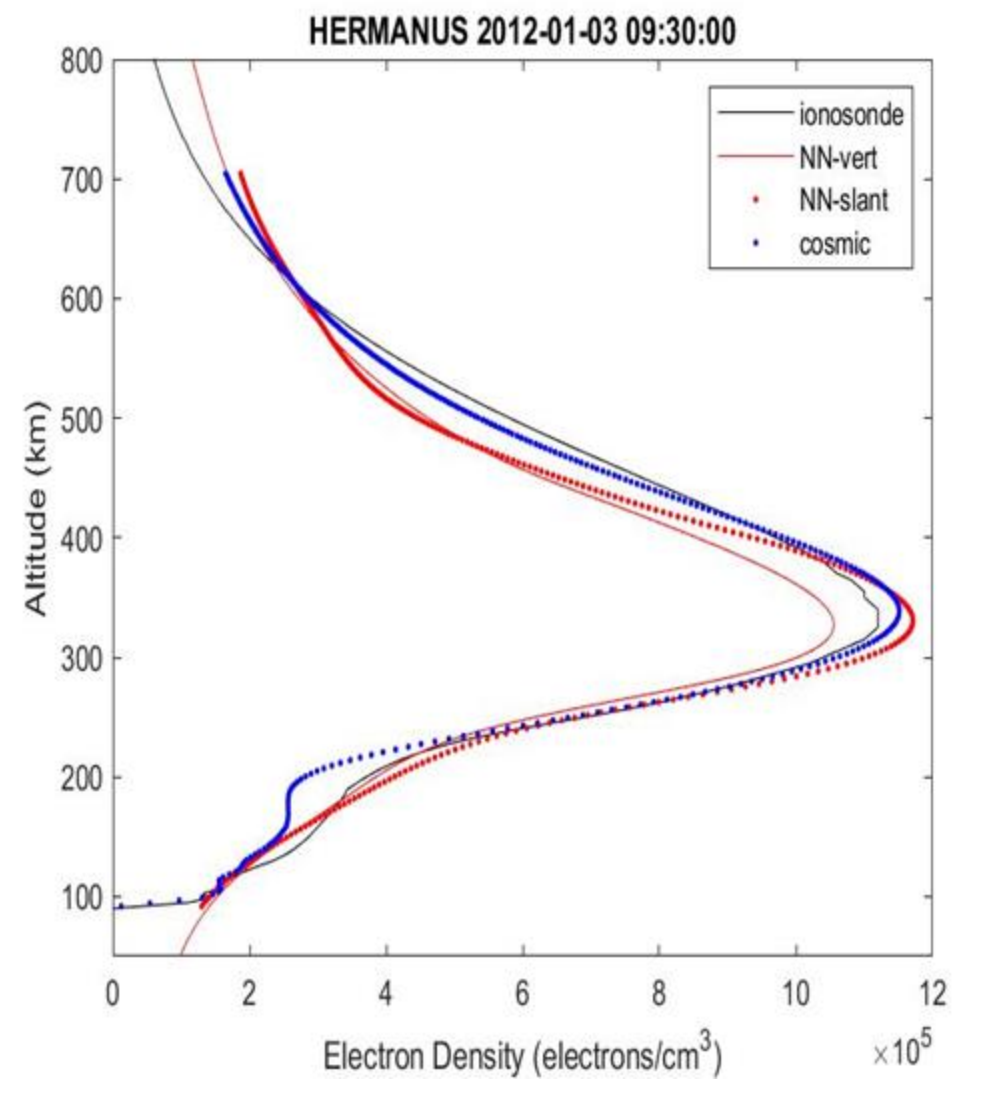
Results; "spatial validation" with independent data source

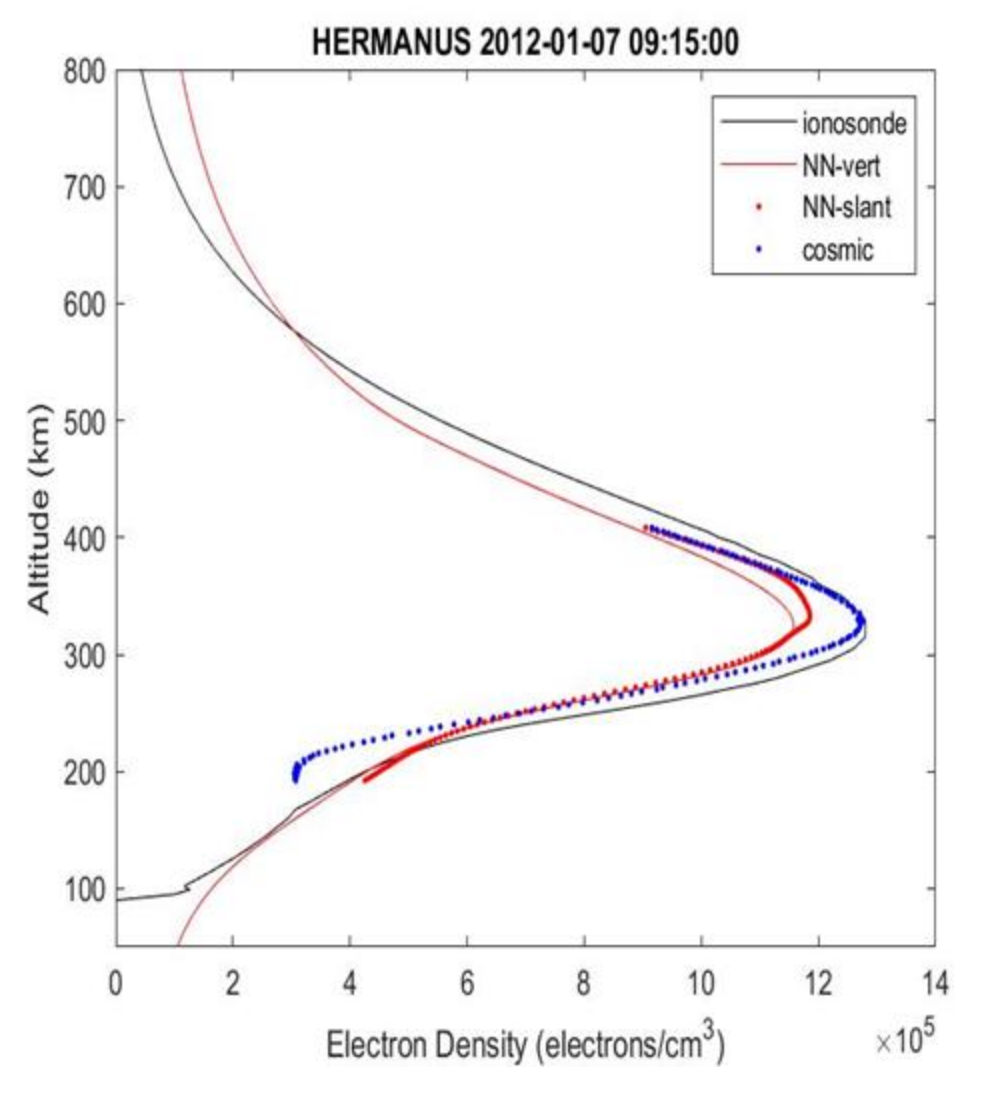




3D-NN model electron density simulations compared to the TEC from Global lonospheric Maps.

Comparing electron density profiles over Hermanus

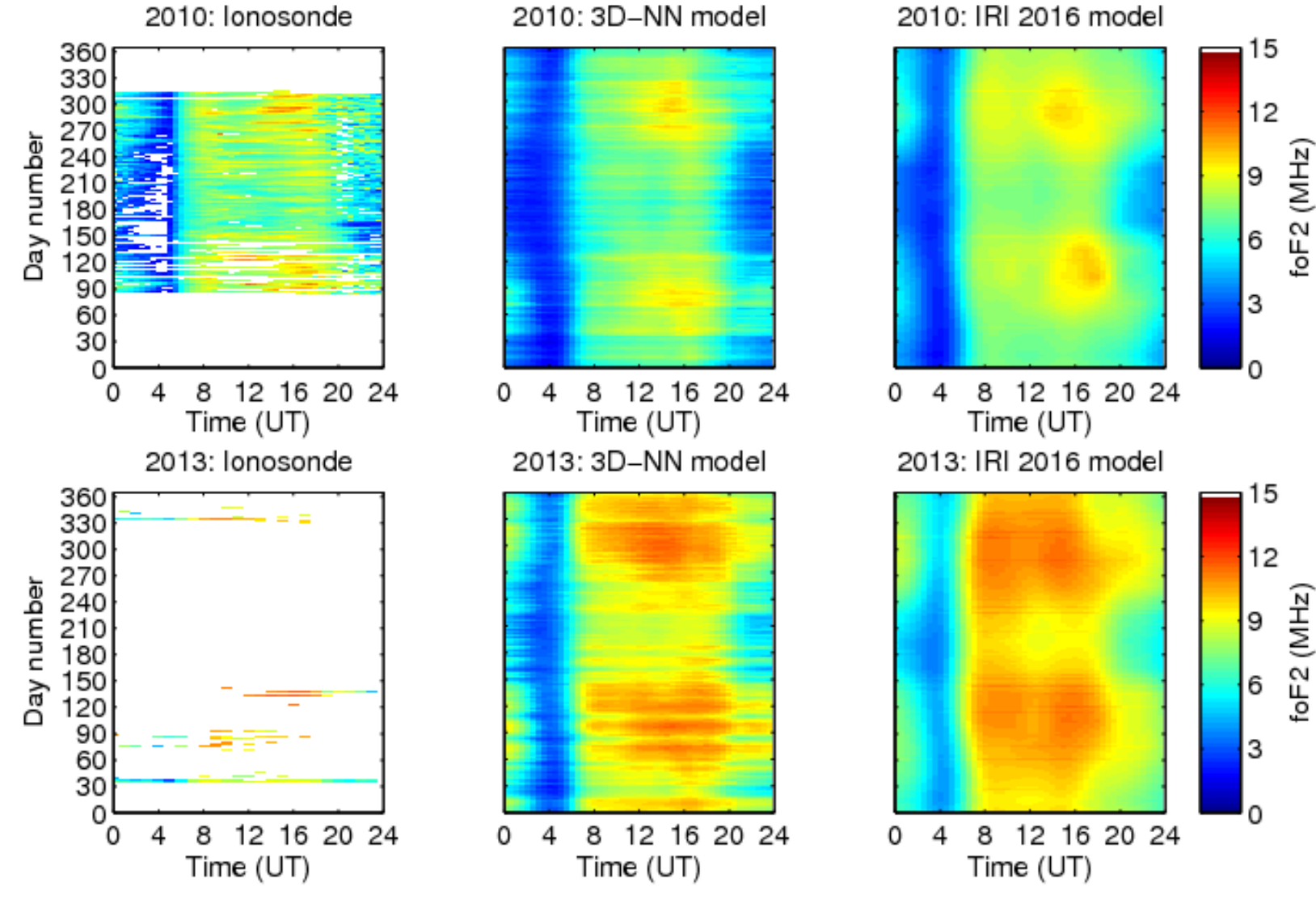








IL008 (1.8°S, geomagnetic latitude)

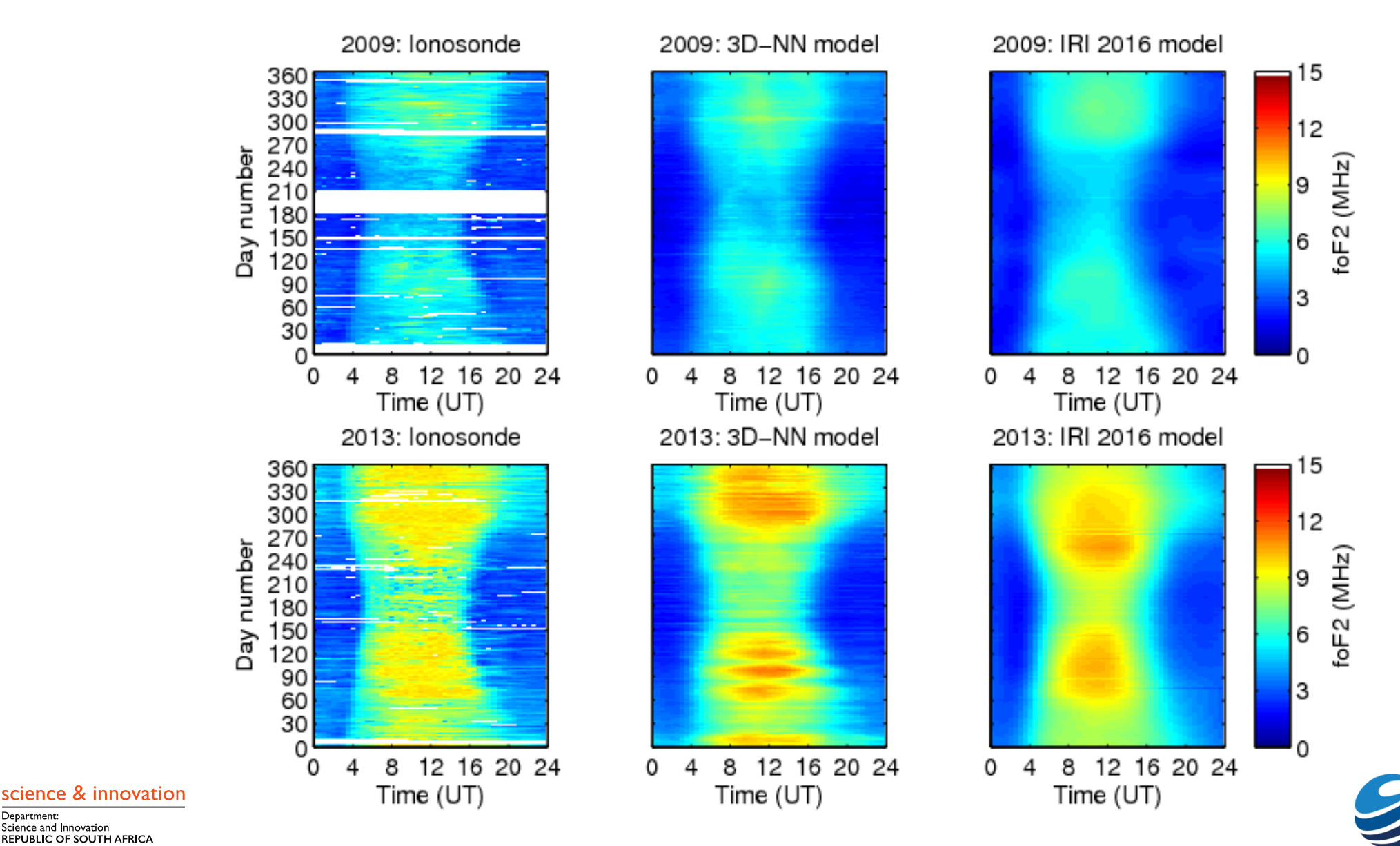




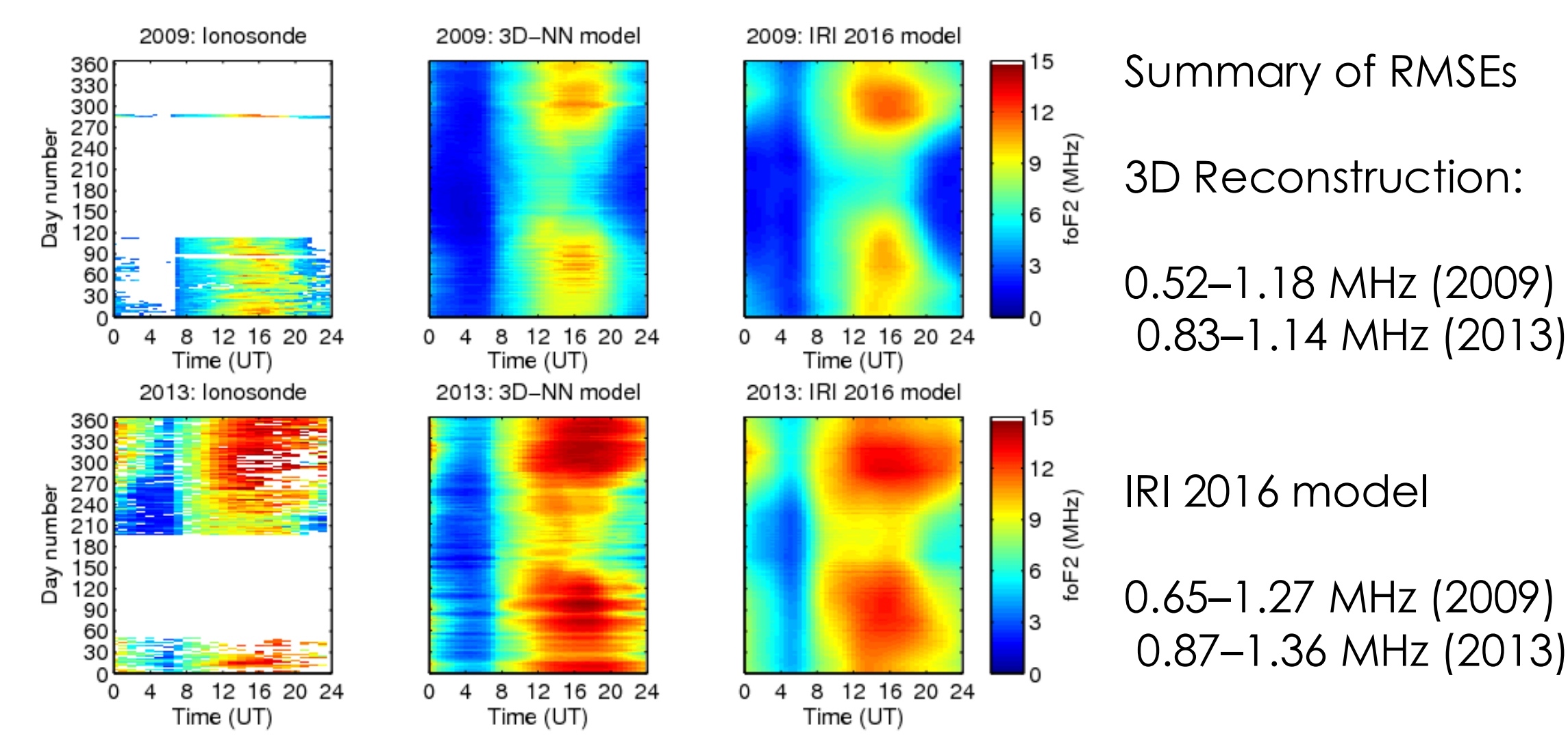


GR13L (42.0°S, geomagnetic latitude)

Science and Innovation REPUBLIC OF SOUTH AFRICA



ASOOQ (12.3°S, geomagnetic latitude)

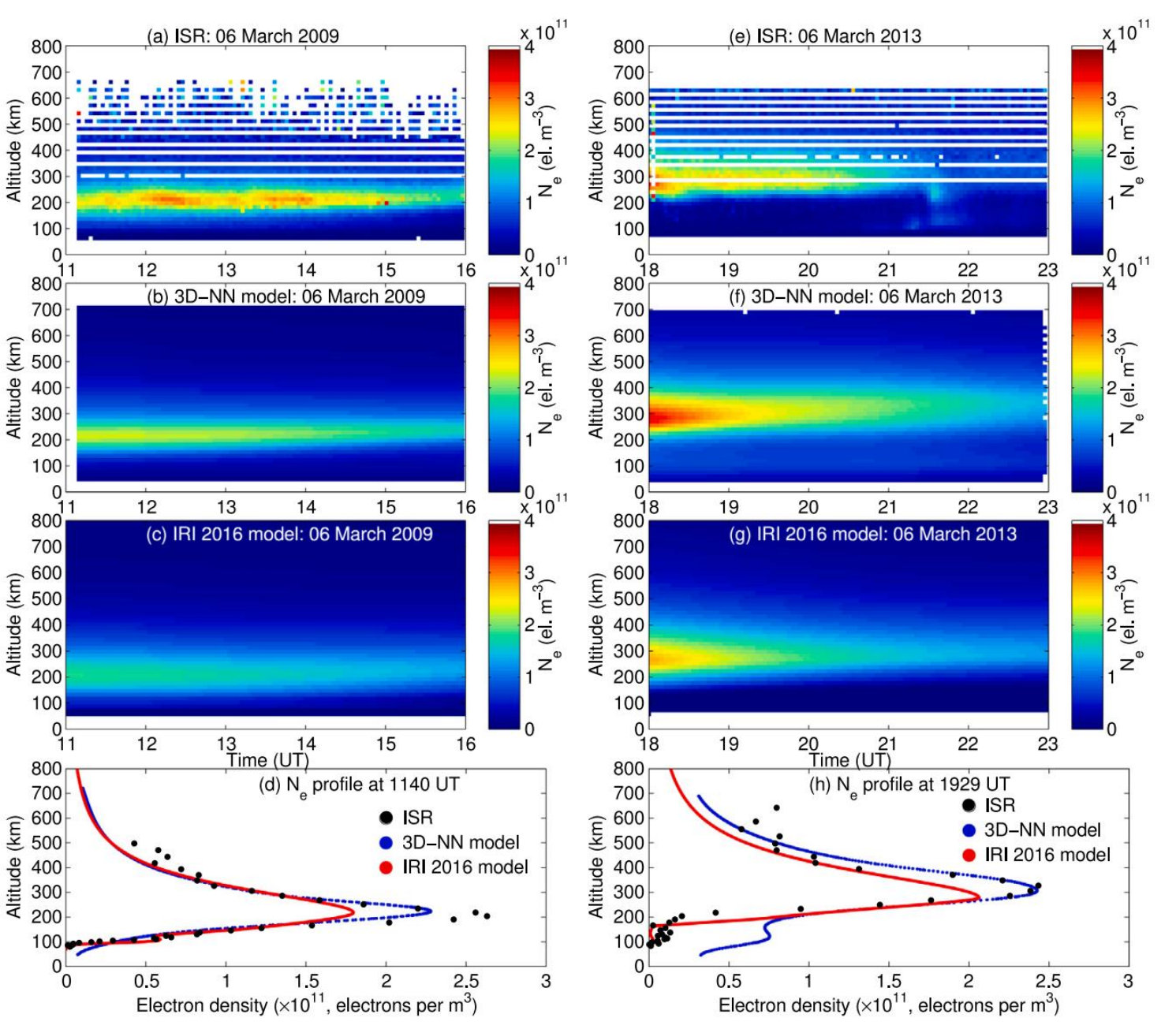


science & innovation



Results over ISR locations: TromsØ (69.6°N, 19.2°E)

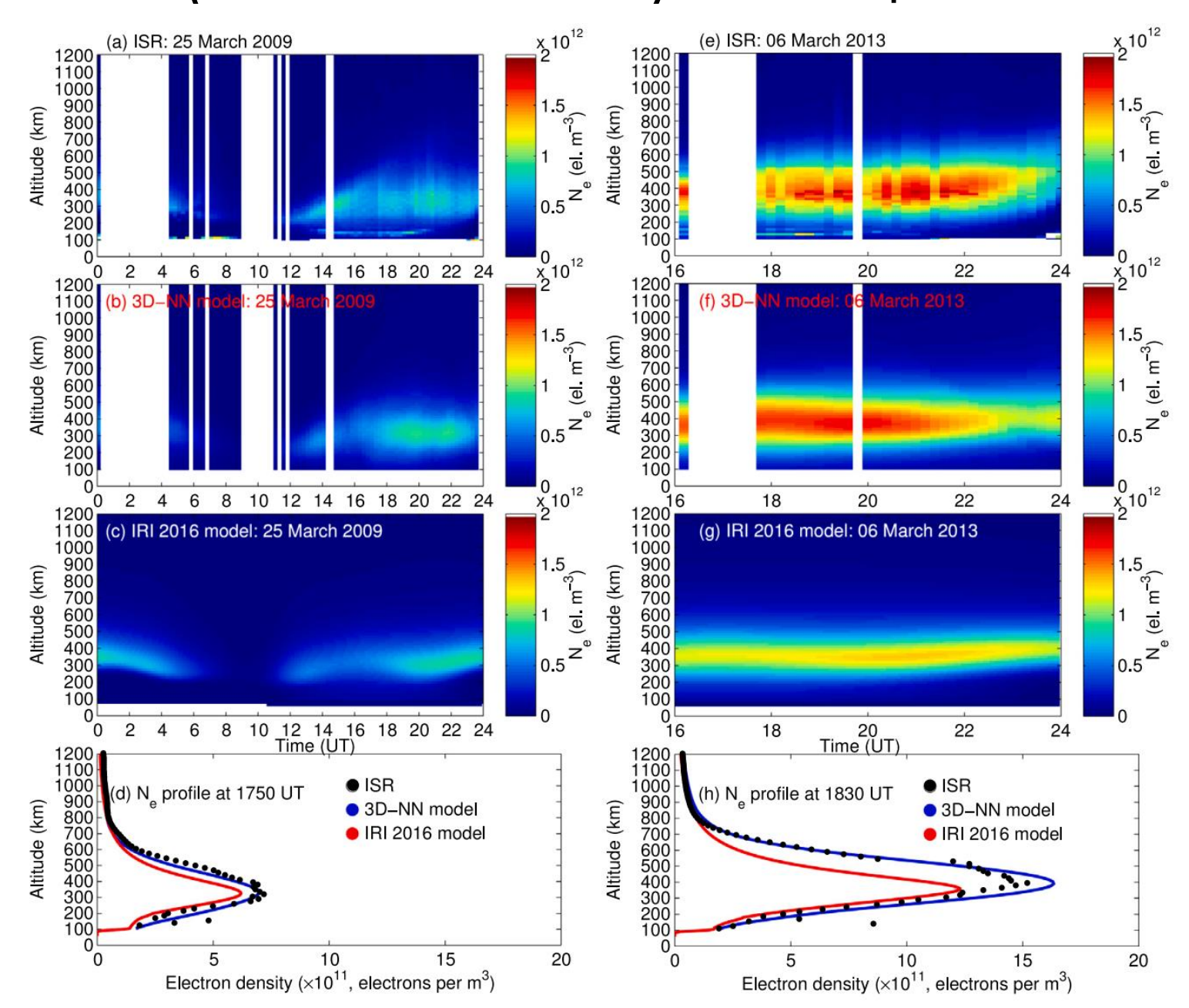
Notice the IRI's Performance at lower altitudes







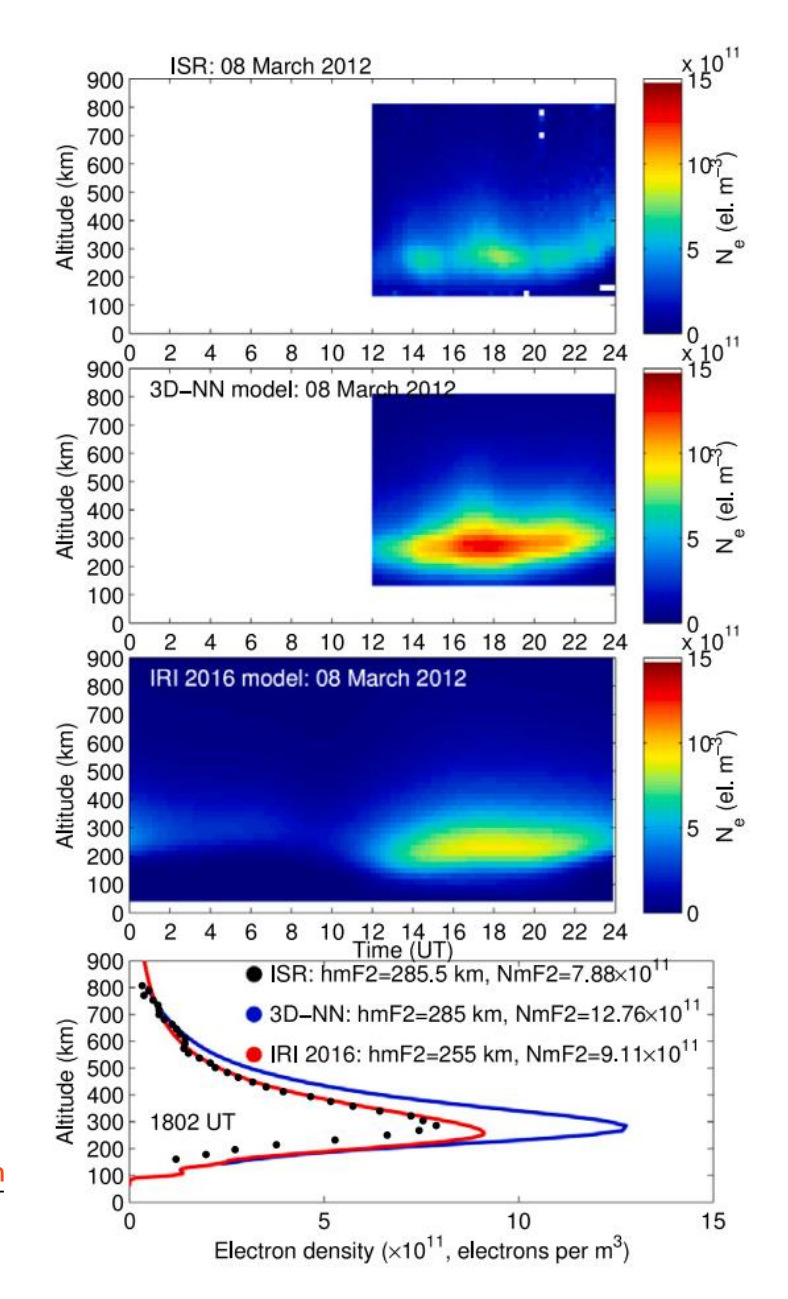
Results over JRO (11.8°S, 77.2°W), an equatorial location

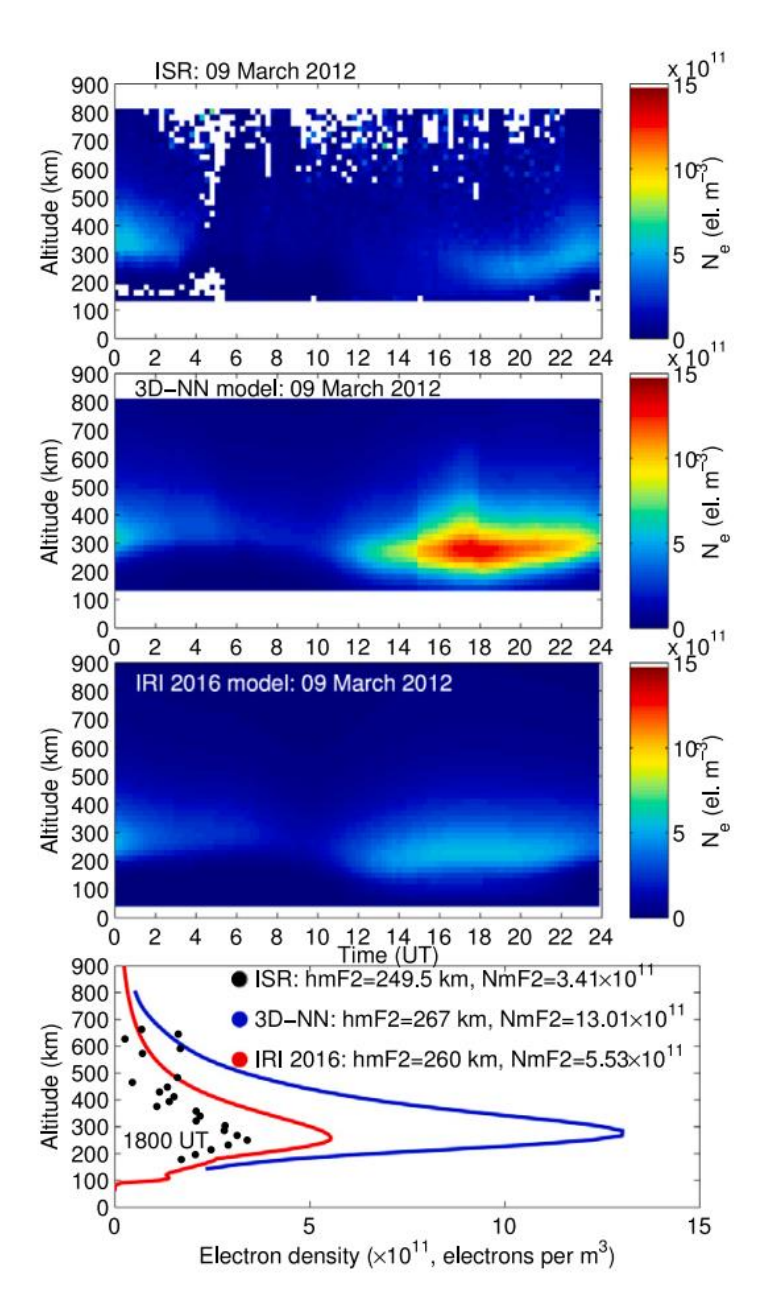






Millstone Hill (42.6°N, 71.5°W) results: storm conditions

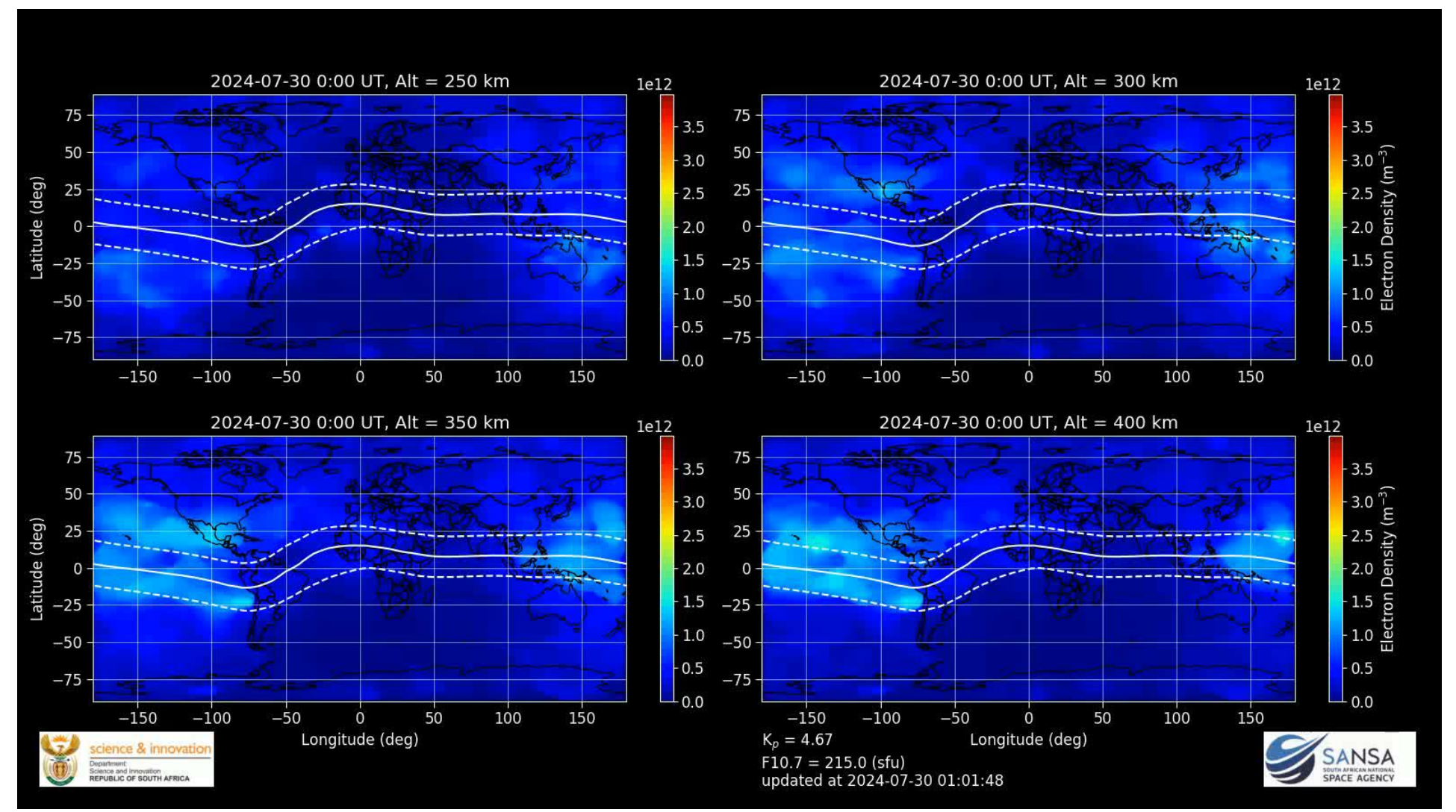








3D-reconstruction background model in real time







Summary of what has been done so far...

The 3D-NN model (developed based only on radio occultation data; COSMIC) reproduces expected ionospheric features

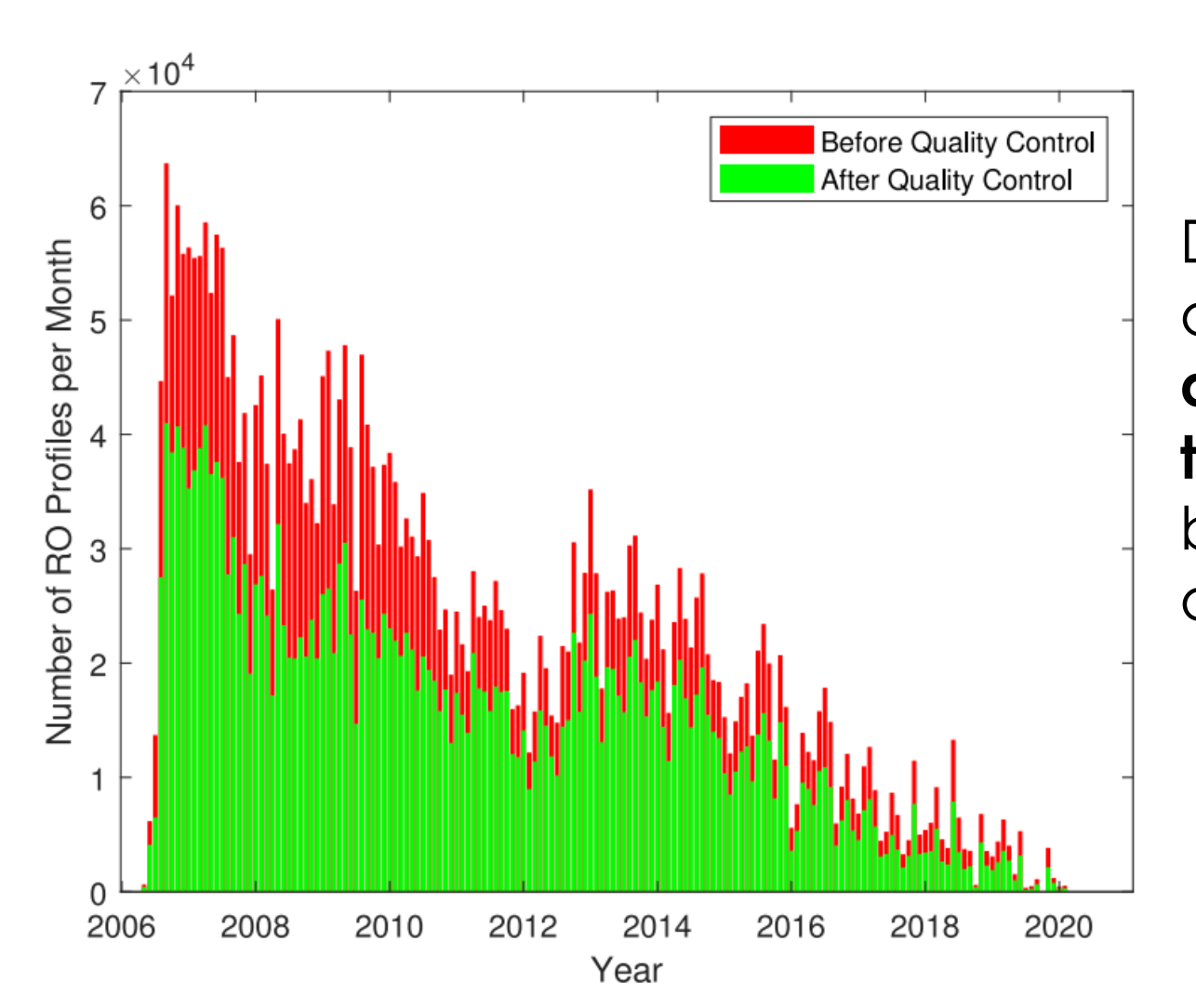
The 3D-NN model's performance during storm conditions is significantly degraded (an expected result) and requires an improvement.

Need to understand the problems of the first model and work towards the solution===which is the next step





Problem with storm time modelling: Amount of quiet and storm time data within the database: Data imbalance that Yenca talked about



During the 3D-NN model development, only 4.4% accounted for the storm-time dataset based on storm criterion of $Kp \ge 4$.





Development of a storm-time model

Construct a storm time dataset for model development. The storm criteria used is $Dst \le -50$ nT and Kp > 4. Two data sources have been considered

COSMIC data: 2006-2021

Ionosonde data: 2000-2020.

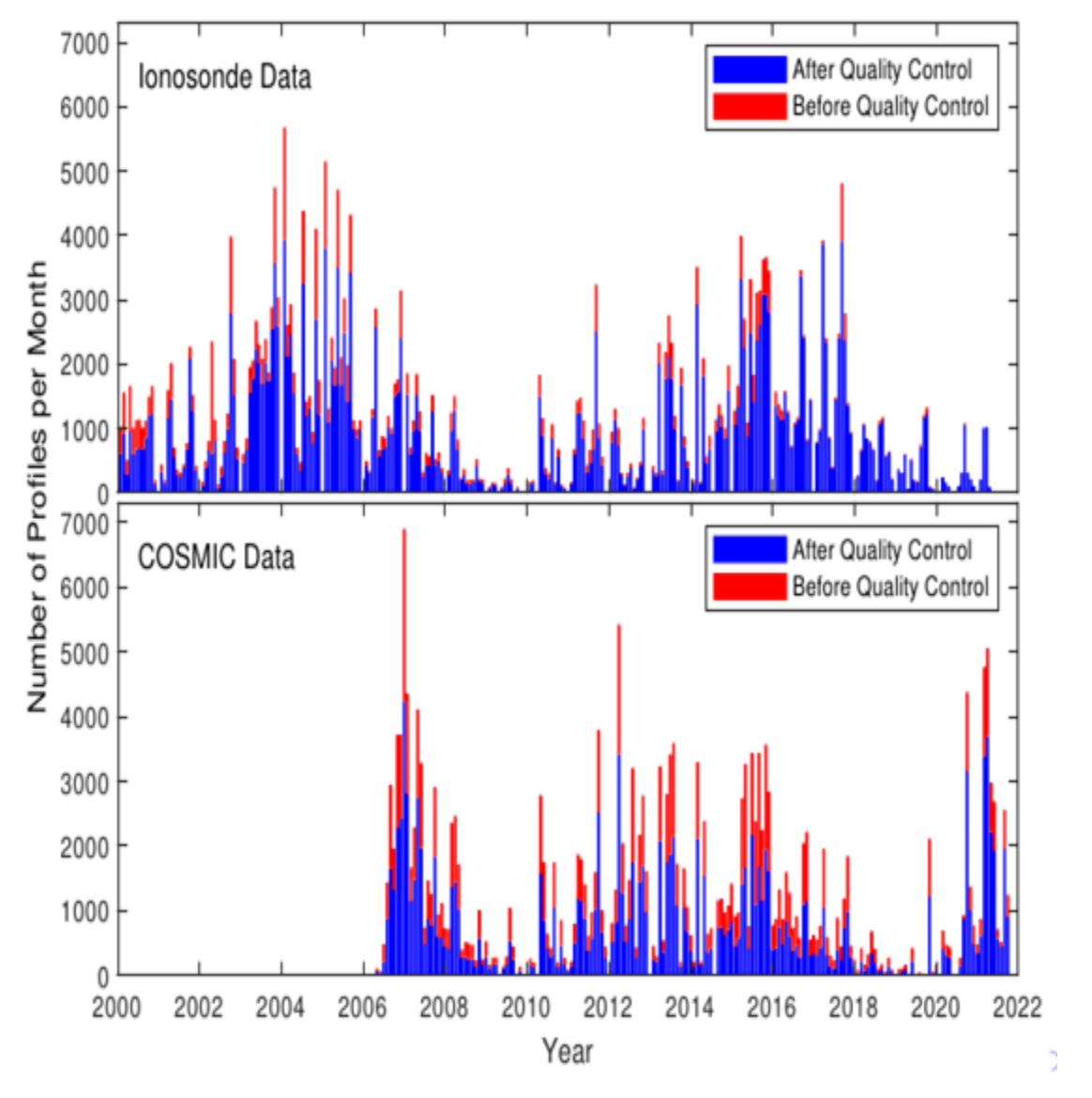
Perform data quality control

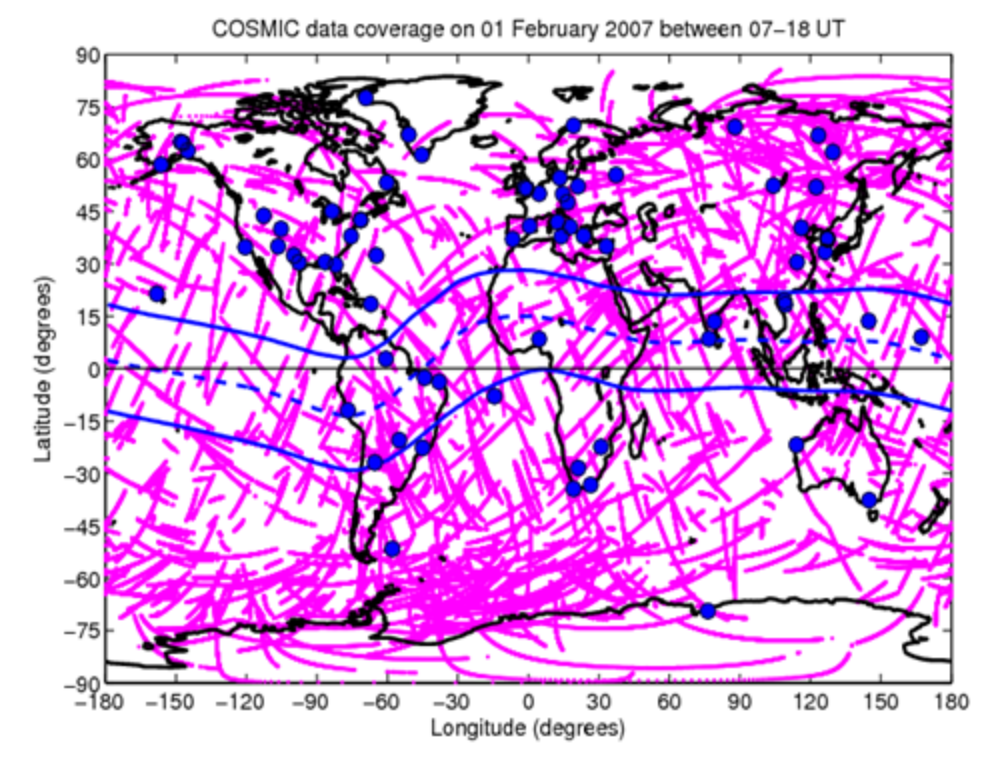
- COSMIC data:= eliminated negative values from electron density profiles;
 == Eliminate Ne profiles exhibiting negative values above 100 km altitude: == Profiles with hmF2 outside the range 200-550 km were also completely eliminated from the database
- Ionosonde data: This dataset has a criteria to assess the confidence level or c-score of auto-scaling software ranging from 0-100%. In this case, 100% represents perfect scaling while the c-score is assigned 0 when the interpretation is obviously wrong. In this study, we selected data for c-score above 70% which acted as the data quality control mechanism





Storm-time data base: Ionosonde and COSMIC datasets





==The storm time model is developed based on COSMIC and ionosonde data (up to hmF2 peak).



==Validation is done on ISR dataset which is completely independent



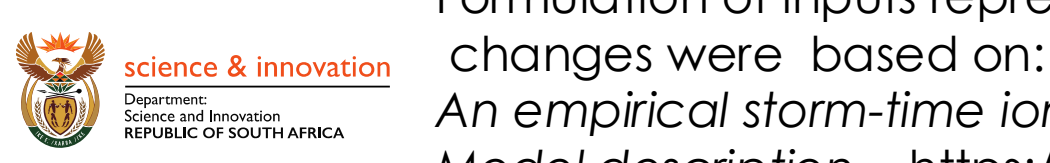
Input space for the storm-time model

Input	Parameterisation used
1. Seasonal Variation	Day number of the year (DoY)
2. Diurnal variation	Hour of the day (HH)
3. Solar activity	Solar flux at 10.7cm wavelength
	(F10.7)
4. Spatial variation	Geographic latitudes and longitudes
Altitudinal variation	Altitude corresponding to
	N_e observations
Current status of geomagnetic activity	Kp and Dst indices
Delayed response of ionosphere due to	$d/dt(Kp (\delta t = 3))$
electric fields of magnetospheric origin	and $d/dt(Dst\;(\delta t=1))$
8. Ionospheric response during the presence	
of atmospheric gravity waves (AGWs)	$d/dt(Kp (\delta t = 9))$
Response due to delayed contribution	
of thermospheric composition changes	$d/dt(Kp (\delta t = 33))$

Physical mechanisms with respect to different time delays

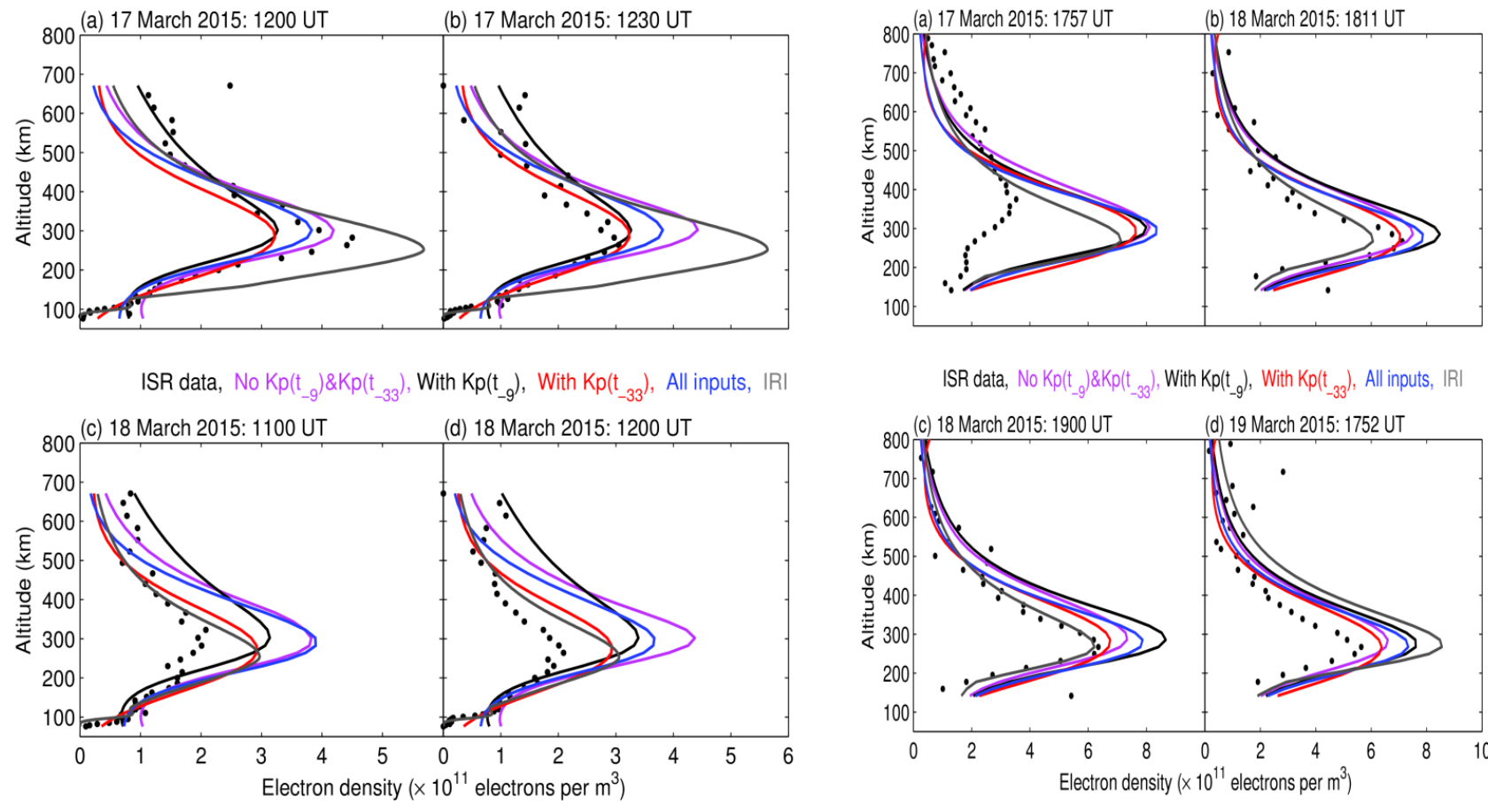
$$\frac{dx}{dt} = \frac{x_{t+\delta t} - x_t}{\delta t}$$

where x is the storm index indicator



Formulation of inputs representing effects of AGWs and neutral composition changes were based on: Araujo-Pradere et al., (2002), STORM: An empirical storm-time ionospheric correction model 1. Model description, https://doi.org/10.1029/2002RS002467.

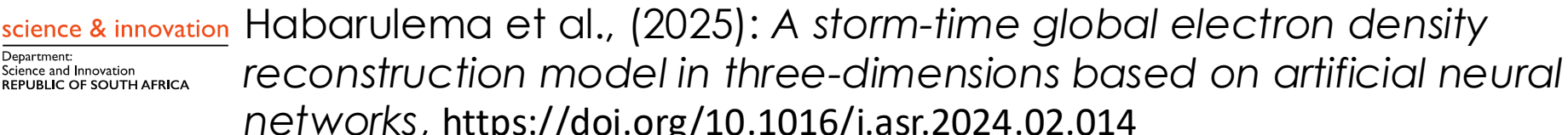
Electron density profiles: Tromso and Millistone Hill



Tromso: The storm time improvement reaches 70% e.g at 1230 UT for the input representing composition changes

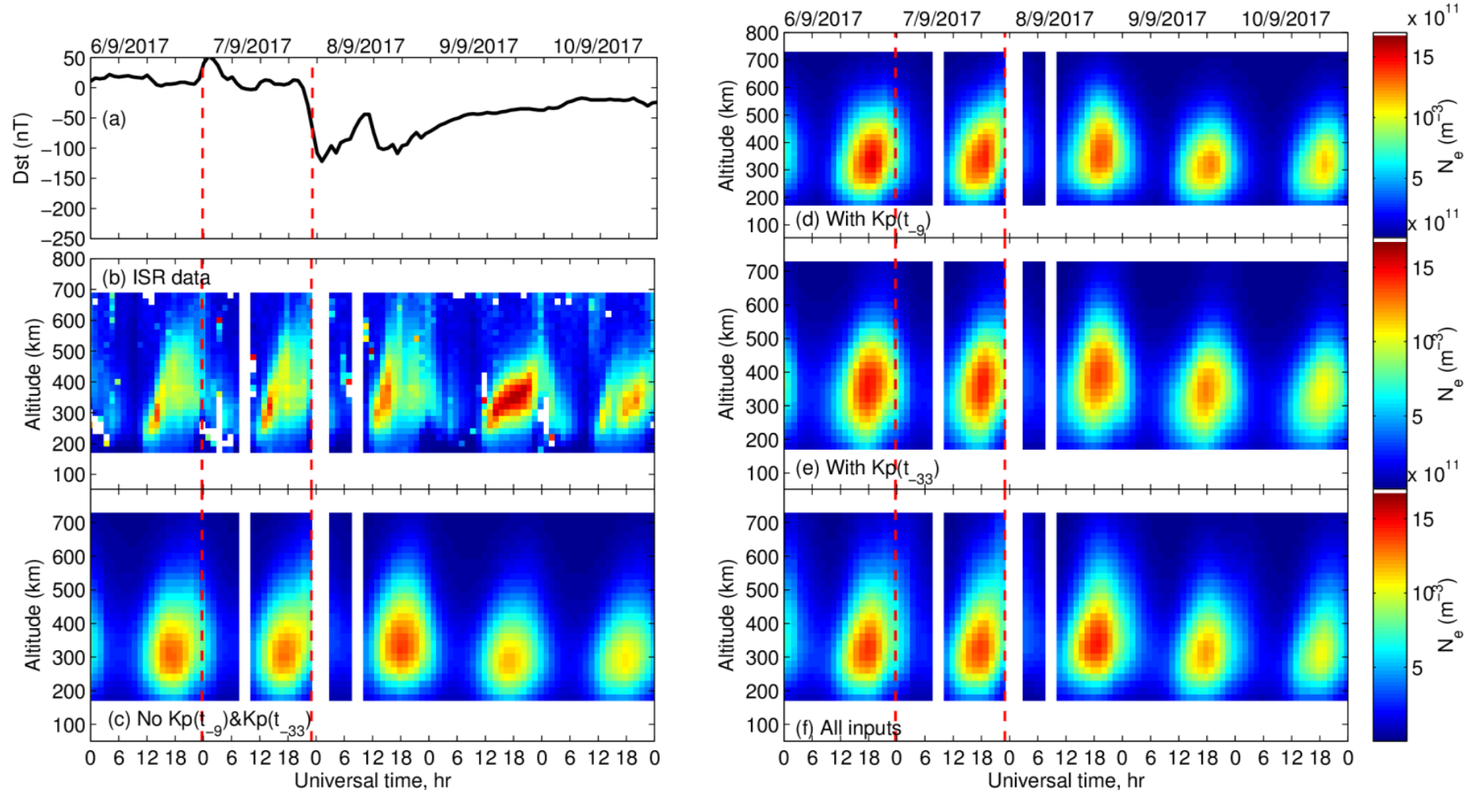
Millistone Hill: IRI 2016 model better by 16% during the main phase while the storm time model does well further







Jicamarca results: 6-10 September 2017 storm



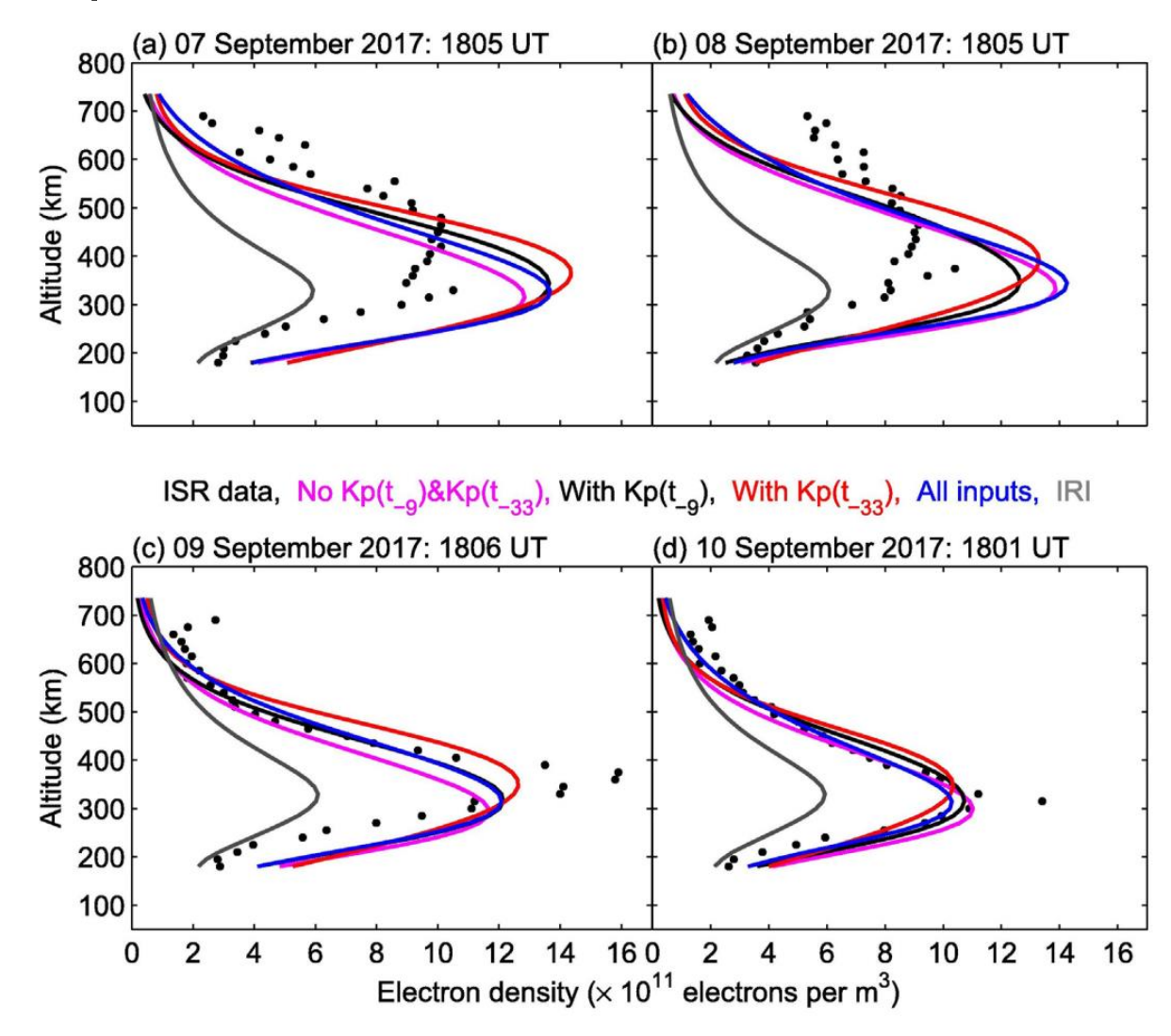
Jicamarca (11.8°S, 77.2°W)

(c): $N_e(3D) \equiv f\left(HH, DoY, Sp, Altitude, F10.7, Dst, Kp, \frac{d}{dt}(Dst), \frac{d}{dt}(Kp)\right)$





Ne profiles over Jicamarca



Habarulema J. B.,, D. Okoh, D. Buresova, B. Rabiu, D. Scipion, I. Haggstrom, P. J. Erickson, and M. Milla (2025): A storm-time global electron density reconstruction model in three-dimensions based on artificial neural networks, https://doi.org/10.1016/j.asr.2024.02.014





Summary

- A quiet time model constructed based on radio occultation data (2006-2019)
- A disturbed time model (developed using a combination of ionosonde (2000-2020) and radio occultation (2006-2021)

AND Many thanks to (for making science research possible)

- COSMIC science and Data teams for making data available (https://data.cosmic.ucar.edu/gnss-ro/)
- 2. Ionosonde data providers to the GIRO Database (https://giro.uml.edu/)
- 3. IRI Model developers (http://irimodel.org/)
- ISR data providers: http://landau.geo. cornell.edu/madrigal/index.html/; http://portal.eiscat.se/madrigal/cgi-bin/gSimpleUIAccessData.py
- 5. Other historical ionosonde dataset: National Geophysical Data Center (https://catalog.data.gov/dataset/ionospheric-digitaldatabase)
- 6. Kp and Dst indices were obtained from https://wdc.kugi.kyoto-u.ac.jp/wdc/Sec3.html
- F10.7 data obtained from https://omniweb.gsfc.nasa.gov/form/dx1.html
- Other data sources that may have been unintentionally omitted (apologies)









